Supramolecular Guanosine 5′-Monophosphate Structures in Solution. Light Scattering Study

Hanna Jurga-Nowak,* Ewa Banachowicz, Andrzej Dobek, and Adam Patkowski

Molecular Biophysics Laboratory, Institute of Physics, Adam Mickiewicz University, Umultowska 85, 61-614 Poznan, Poland

Received: July 23, 2003; In Final Form: November 4, 2003

During the past decade, from the vast evidence it became clear that DNA oligomers rich in guanine stretches can form in solution highly ordered forms called G-quadruplexes and G-wires. G-quadruplexes are present in many sites of the human genome, can inhibit telomerase, and can be used as drug delivery supramolecules. G-wires and related structures seem to be an excellent material of biological origin for nanostructures. Therefore, in this paper we have studied the structures formed by specific association of guanosine 5′-monophosphate (GMP) nucleotide molecules in water solutions by photon correlation spectroscopy and depolarized Rayleigh light scattering. One relaxation process with distinct amplitude was observed, as a function of temperature and sample concentration. It was attributed to the translational diffusion coefficient of the stacks of G-quartets in a range of high concentration and to the stacks of GMP monomer associates for low concentration (less than 40 mg/mL). From the measurements the hydrodynamic radius of GMP molecule has been estimated as $r_H \simeq 5.4$ Å. The bead modeling of the hydrodynamic parameters allowed us to distinguish the wide spectrum of structures formed in solution: from single GMP nucleotides to stacks of multiassociates of G-quartets of GMP.

I. Introduction

From the beginning of the 1970s, attempts at explaining the ability of guanosine 5′-monophosphate (GMP) to self-organize, unusual among other DNA and RNA nucleotides, have been made on the basis of X-ray diffraction,[1−5] nuclear magnetic resonance,[6] Fourier transform infrared spectroscopy,[7] and circular dichroism experiments.[8] The basis for the data interpretation was the assumption, later experimentally confirmed, that GMP forms the so-called G-quartets. The G-quartet consists of four planar guanine molecules, arranged in a cyclic pattern, bound by double hydrogen bonds in the Hoogsteen manner between N_1-O_6 and N_2-N_7 of successive guanines (Figure 1a). The stacks of G-quartets (Figure 1b), stabilized by the stacking interactions, form G-quadruplexes whose structure resembles that of four-stranded B-DNA. At the center of the G-quartet is a cavity formed by O_6 ketone groups. It is a coordination site of metal ions in the plane of the G-quartet[9] or between adjacent G-quartets.[10,11] Formation of the ordered structures of GMP sodium salt (Na_2GMP) [12] and the influence of ions such as K^+, Na^+, Rb^+, Cs^+, Li^+, NH_4^+, and $(TMA)^+$ on the structure and its size have been investigated by many authors[9−11,13−15] using NMR technique. The ability of the monovalent cations to promote G-quartet structure formation decreases in the order $K^+ \gg Rb^+ > NH_4^+ > Na^+ > Cs^+ > Li^+$, whereas the ability of divalent ions to stabilize these structures decreases in the order $Sr^{2+} \gg Ba^{2+} > Ca^{2+} > Mg^{2+}$.[16,17] The interest in structures formed by guanine nucleotides increased with the finding that some regions of chromosomal DNA are rich in guanine sequences. These are immunoglobulin switch regions,[18,19] gene promoter regions,[20,21] P1 promoter for c-myc oncogene regions,[22] fragile X syndrome repeats,[23] insulin linked polymorphic regions,[24,25] and telomers.[26−28] It was also observed that G-quartets might significantly affect the functioning of a single living cell.

The above-mentioned methods allowed a detailed description of the local structure and conformation of the G-quartets. Unfortunately, they did not offer a possibility of investigating the size and shape of those structures in solution. Such a possibility is offered by dynamic light scattering measurements of the translational and rotational diffusion coefficients. These parameters allow determination of the hydrodynamic radius of the structures as a function of temperature, ionic strength, and nucleotide concentration. Photon correlation spectroscopy techniques (PCS) were applied for the first time in the early 1990s by Eimer[29] to study the influence of sodium ions on the self-aggregation ability of Na_2GMP. Measurements of the translational and rotational diffusion coefficients as a function of temperature, GMP concentration, and ionic strength allowed an estimation of the dimensions and shape of the structures formed. Depending on the conditions in solution, Na_2GMP created associates of nine-stacked G-quartets or stacks of four GMP monomers.

We used the method of dynamic light scattering and the bead modeling of the hydrodynamic parameters to determine the size of the structures formed by GMP (guanylic acid) mononucleotides. The method is a noninvasive technique allowing a study of the dynamics of a macromolecular system. The changes in the diffusion coefficient value are related to those in the shape and size of the molecules, and thus to the interactions between them leading to formation of more organized structures.

II. Experimental Section

Materials. The sample of lyophilized guanosine 5′-monophosphate (5′-GMP, $C_{10}H_{14}N_5O_8P$, $M_w = 363.2$) from yeast was purchased from Sigma-Aldrich GmbH. The purity of the compound was >98%, so it was used without further purifica-

* Corresponding author. Telephone: 48-61-8295-257. Fax: 48-61-8295-167. E-mail: hjurga@amu.edu. pl.

10.1021/jp030905+ CCC: $27.50
Published on Web 01/29/2004

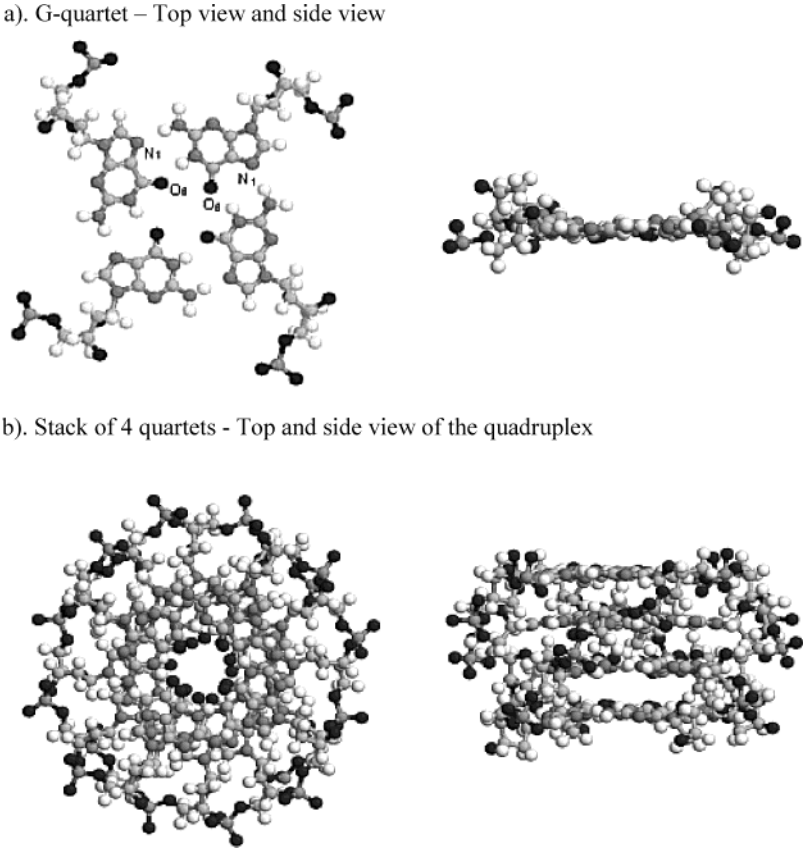

Figure 1. Structure of (a) G-quartet (G-tetrad), shown from the top and side. N_1 and O_6 atoms of the guanine molecule participating in double hydrogen bonds in the Hoogsteen manner are indicated. (b) Structure of stack of four G-quartets (tetrads), shown from the top and side, with characteristic cage in the center. The carbon atoms are light gray, nitrogen atoms are dark gray, oxygen atoms are black, and hydrogen atoms are white.

tion. The samples of 5′-GMP were prepared by dissolving the GMP in distilled, deionized, and filtered water or in 10 mM Tris buffer [Tris(hydroxymethyl)aminomethane, $C_4H_{11}NO_3$, M_w = 121.1] (pH 7.3) containing differing molarity of sodium chloride (NaCl). The water used for buffer preparation was deionized (by means of deionizer EASYpure RF, Barnstead), and the buffer itself was filtered (0.22-μm Millipore, Milex-GV: SLGV013SL and SLGV004SL filters) before making the GMP solutions. The solution sample was again filtered into a quartz fluorescence cell (Hellma, Catalog No. 111.057QS). The sample concentration was determined from absorption measurements at λ = 260 nm (spectrophotometer UV−vis M-42, Carl Zeiss Jena), and the experimentally determined molar extinction coefficient ϵ_{260} = 10 674 $[M\cdot cm]^{-1}$ was used for calculations. The sample was centrifuged for 20 min at 6700 *g* to reduce the air bubbles. The sample was stored at room temperature, at which it was characterized by very good water solubility. At lower temperatures GMP underwent self-aggregation leading to gel formation. The process of heating and subsequent cooling of the samples of concentrations higher than 110 mM (40 mg/mL) led to GMP precipitation in the form of small white balls. The efforts of dissolving GMP in 50, 75, or 100 mM water solutions of sodium salt (NaCl) ended with immediate gel formation. The GMP solubility in 10 mM Tris buffer with small amounts of NaCl was good, and no gel formation was observed at room temperature. However, after 2 days all GMP solutions exhibited irreversible precipitation and the sample lost its monodispersity and transparency.

Methods. *Photon Correlation Spectroscopy*. Translational and rotational motion of the molecules in solution leads to concentration fluctuations, manifested in the time dependence of the scattered light fluctuation intensity. The homodyne, normalized time correlation function of the scattered light intensity, is given by

$$g_2(\tau) = 1 + \beta \exp(-2q^2 D_T \tau) \quad (1)$$

where D_T is the translational diffusion coefficient, β is the product of the instrumental constant and the contribution of the density fluctuation in the total intensity of the scattered light, and q is the magnitude of the scattering vector expressed by

$$q = \frac{4\pi n}{\lambda_i} \sin\frac{\theta}{2} \quad (2)$$

where n is the refractive index of the solution, λ_i is the wavelength of the incident light, and θ is the scattering angle. The translational diffusion coefficient D_T and the value of the scattering vector q are related to the correlation function exponential decay rate Γ through the formula

$$\Gamma = q^2 D_T \quad (3)$$

The experimental correlation function was analyzed using a double exponential according to the general equation

$$g_2(\tau) = [\sum_{i=1}^{n} A_i \exp(-\Gamma_i \tau)]^2 + 1 + s(\tau) \quad (4)$$

where A_i is the ith process contribution, Γ_i is the correlation function decay constant, n is the number of diffusive processes, and $s(\tau)$ is an unknown small background correction. The fitting

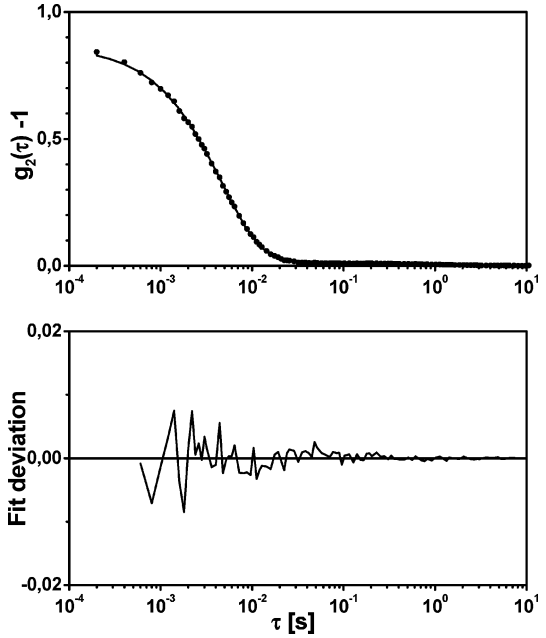

Figure 2. Time correlation function for the GMP in water solution, pH 2, $c = 260$ mg/mL, and $T = 50$ °C. The DISCRETE double-exponential fit and residua are shown.

program DESCRETE by Provencher[30] was used. It allowed a fit of the sum of exponentials to the correlation function and optimization of the number of decay functions to two sets of the best solutions. The example of time correlation function is given in Figure 2. At first the correlation function was analyzed using another fitting program, CONTIN. The fits have shown that we deal with monodisperse solution. Using CONTIN, we were not able to find more than one significant component. Because of that, for the final analysis we decided to use DISCRETE, which works well at analyzing correlation functions coming from solutions with well separated components. The fits obtained by means of CONTIN and DISCRETE are close; however, CONTIN gives a slightly smaller value of the translational diffusion coefficient (the difference does not exceed 2%).

Rayleigh Light Scattering: Depolarized Component Measurements. The anisotropic part I_{VH} of the total intensity of the scattered light, polarized perpendicularly with respect to the incident light beam, depends on the molecule's anisotropy and on the intermolecular orientation correlations. The depolarized component I_{VH} can be exploited, among others, to reckon the optical anisotropies of the chain molecules in the solution and to relate them to the conformations of these molecules.[31] In the ordered medium the mean anisotropy of the optical polarizability can show higher values with respect to the disordered medium. The measurement of the I_{VH} component as a function of temperature gives information about the degree of ordering of the molecules in the solution.

Apparatus. The experimental setup for light scattering experiments consisted of an argon ion laser (ILK120 by Carl Zeiss Jena, $\lambda = 488$ nm, output power 400−800 mW), a goniometer with 0.1° accuracy (ALV/SP-125 SN46, ALV GmbH, Langen) and a digital correlator (ALV-5000 Multiple Tau Digital Correlator, ALV, Langen). The small molecules, in a range of low concentrations, were investigated, so for all measurements the maximum power of the focused laser beam was used (focal length $f = 40$ cm). The measuring cell was thermostated and temperature was kept constant within ±0.1 °C. A system of two photomultipliers ALV/SO-SIPD/DUAL and simple photon detector, working in the regime of photon counting, was used as a detector. The photomultiplier was placed on the goniometer arm, and the light scattered at 90° angle was collected by means of a single-mode optic fiber. The photon correlation function of the scattered light was obtained by using the digital correlator (ALV GmbH, Langen). In the depolarized scattered light measurements, the depolarized component of scattered light intensity was selected by the Glan-Thompson analyzer and the ALV correlator was used to collect the light intensity I_{VH}.

TABLE 1: Comparison of Translational Diffusion Coefficients D_{T20} Calculated for Stacks of Different Numbers n of G-Quartets (G-Tetrads) Assuming Bead and Cylindrical Models ($L = 3.4n$ Å, $d = 26$ Å; L = Length, d = Diameter of the Cylinder)

	bead model	cylindrical model	
n	D_T (10^{-6} cm^2/s)	D_T (10^{-6} cm^2/s)	$p = L/d$
1	2.136	71.46	0.131
2	1.957	12.20	0.262
3	1.844	5.008	0.392
4	1.705	3.044	0.532
5	1.572	2.270	0.654
6	1.493	1.888	0.785
7	1.426	1.666	0.915
8	1.364	1.521	1.046
9	1.277	1.417	1.177
10	1.222	1.337	1.308
11	1.181	1.272	1.438
12	1.150	1.218	1.569
16	1.012	1.061	2.092
24	0.815	0.868	3.138
32	0.710	0.746	4.185

III. Results and Discussion

Bead Model. Eimer and Dorfmüller[29] have applied the cylindrical model to approximate the shape of the observed associates of sodium salts of GMP in water solutions of different sodium chloride contents. The cylindrical model is used for characterization of the elongated shape structures (rod structures) and has been found suitable for the description of many small biomacromolecules, such as oligonucleotides or short segments of DNA. The authors assumed hydrodynamic properties of the molecule of cylindrical symmetry with small $p = L/d$, where L is the length and d the diameter of the cylinder. Such an approach was proposed by Tirado and Garcia de la Torre, and can be used only for $2 \leq p \leq 30$ (the Tirado−Garcia de la Torre condition[32,33]). This condition is not fulfilled for very short DNA segments, for stacks composed of a few G-quartets, or for stacks of a few single GMP nucleotides. In contrast to the cylindrical model, the bead model can be applied without limitations as to the molecule shape and size. Therefore, we used the bead model for calculation of the hydrodynamic parameters describing the structures observed. A comparison of the translational diffusion coefficients calculated for stacks of quartets assuming the two models discussed above (Table 1) shows that, only for stacks of over 16 G-quartets ($2 \leq p \leq 30$), the coefficients deduced from both models are similar. The Tirado−Garcia de la Torre condition is also fulfilled for associates of single GMP monomers larger than a six-nucleotide stack (Table 2). It looks as though the bead model, working in a wide range of sizes of the structures observed, is much more universal.

The translational diffusion coefficients were calculated for the particular model structures using the HI4 program courtesy of Richard Pastor. The structures of G-quartet stacks were designed by means of the Hyper-Chem program in the bead model. For calculations of the hydrodynamic parameters the

TABLE 2: Comparison of Translational Diffusion Coefficients D_{T20} Calculated for Stacks of Different Numbers *n* of GMP Monomers Assuming Bead and Cylindrical Models ($L = 3.4n$ Å, $d = 10$ Å; L = Length, d = Diameter of the Cylinder)

	bead model	cylindrical model	
n	D_T (10^{-6} cm^2/s)	D_T (10^{-6} cm^2/s)	$p = L/d$
1	3.977	17.460	0.34
2	3.454	5.650	0.68
3	2.898	4.019	1.02
4	2.664	3.405	1.36
5	2.468	3.047	1.70
6	2.272	2.791	2.04
7	2.113	2.613	2.34
8	1.958	2.426	2.72
9	1.85	2.287	3.06
10	1.757	2.166	3.40
11	1.676	2.060	3.74
12	1.604	1.965	4.08

GMP nucleotide was approximated by two identical, partially overlapping beads,[34] each of radius $\sigma = 4.75$ Å. One bead represented the base of the nucleotide and one represented the sugar and phosphate group. The centers of the spheres (beads) were placed at the geometric centers of the groups of atoms belonging to the base and to the sugar and phosphate moieties, respectively. The computer programs for constructing the bead models based on atomic coordinates were written in Turbo Pascal for DOS. The source code of the program NUKLEO3 and its executable version is available on request from the corresponding author. The source code of the HI4 program was modified for the bead model case of partially overlapping spheres by applying the Rotne−Prager interaction tensor.[35] The bead radius was chosen in such a way that the simulated value of D_T for single GMP nucleotide was the closest to the experimental one obtained in water solution for a very small concentration ($c = 20$ mg/mL), Figure 3. The stick boundary conditions for adjacent beads were applied, and the hydrodynamic radius of the nucleotide was calculated at 20 °C using the following expression:

$$r_H = \frac{k_B T}{6\pi\eta_0 D_T} \tag{5}$$

where k_B is theBoltzmann constant and η_0 is solvent viscosity.

The value of the translational diffusion coefficient obtained from linear regression of the measured points (Figure 3a) was $D_T = (3.933 \pm 0.241) \times 10^{-6}$ cm^2/s (which used in eq 5 gave $r_H = 5.43 \pm 0.33$ Å), and the value calculated using the bead model was $D_T = (3.977 \pm 0.266) \times 10^{-6}$ cm^2/s ($r_H = 5.37 \pm 0.36$ Å). As follows from Figure 3a, for the lowest concentration measured (20 mg/mL), there is no temperature dependence of D_T. This observation supports the conclusion that the presence of one kind of structure is observed in the solution under these conditions and these structures are GMP monomers. This result is in good agreement with D_T obtained for 5′-GMP by Rymden and Stilbs[35] from the pulse gradient spin−echo (NMR) measurements. The authors estimated this value extrapolated to zero concentration and viscosity of water at 20 °C to be $D_{0T20} = 3.97 \times 10^{-6}$ cm^2/s.

Hydration of the GMP Molecule. Each GMP molecule in water solution is hydrated, which means that it is coordinatively bonded with surrounding water molecules. The concept of the hydration sphere is arbitrary, and it is understood as a layer of water molecules adjacent to the macromolecule. For the protein or nucleic acid macromolecule, the velocity of their translational motions is the same as that of the water molecules forming the

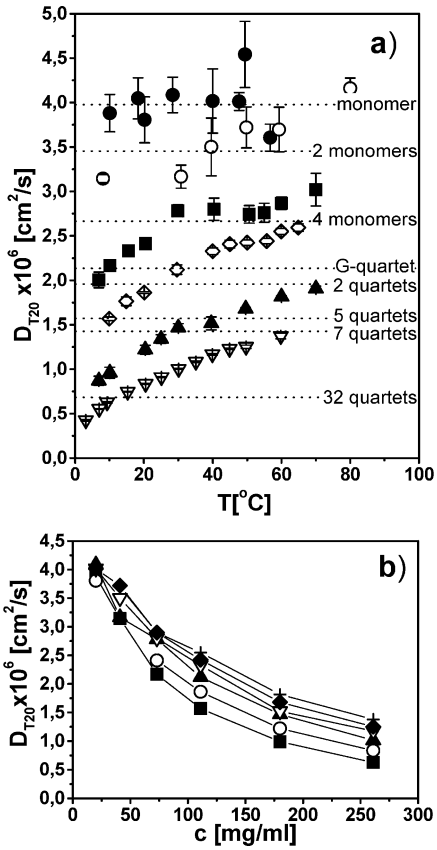

Figure 3. Translational diffusion coefficients D_{T20} as a function of (a) temperature *T* for different GMP concentrations *c* in water solution, pH 2: (●) 20, (○) 41, (■) 73, (◇) 111, (▲) 180, and (▽) 261 mg/mL; (b) GMP concentration *c* for different temperatures *T* in water solution, pH 2: (■) 10, (○) 20, (▲) 30, (▽) 40, (◆) 50, and (+) 60 °C.

hydration sphere. The thickness of such a sphere is assumed to be 3−4 Å. The volume of the hydrated macromolecule is a sum of the volume of the nonhydrated molecule and the volume of the water bound and is expressed by the following formula:[36]

$$V_h = \left(\frac{M}{N_0}\right)(\bar{V}_2 + \delta_1 \bar{V}_1) \tag{6}$$

where M is the molecular weight of the DNA or the protein macromolecule; N_0 is the Avogadro number; $\bar{V}_2 = 1/\rho$ is the partial specific volume of the macromolecule, where $\rho = M/(N_0 V_M)$ denotes the density and V_M is the entire volume of the macromolecule; δ_1 describes the hydration (how many grams of H_2O accounts for 1 g of nucleic acid or 1 g of the protein), and $\bar{V}_1$ (=1 cm^3/g) is the partial specific volume of water molecule.

The volume of a "dry" GMP molecule, calculated on the basis of the bond lengths and van der Waals radii of atoms, is $V_{GMP} = 251.06$ Å^3, and its molecular weight is $M_w = 363.2$ g/mol. The partial specific volume of GMP is $1/\rho = 0.42$ cm^3/g.The radius of a sphere of a volume equal to that of the nonhydrated GMP molecule is $r = 3.91$ Å. It is known that in the B-DNA structure guanine base is bound to three water molecules,[37] one in the minor groove of DNA in the vicinity of N3 atom and two others in the major groove in the vicinity of O6 and N7 atoms. A high concentration of water molecules is observed in the proximity of O1P and O2P atoms of the phosphate groups. In double-stranded DNA, the phosphate group has three hydration sites being the bonding sites of six H_2O molecules.[38] Relative hydration per a single GMP nucleotide amounts to

5−12 water molecules.[39] Using eq 6, one can calculate the hydrodynamic radius of the GMP monomer with five water molecules as $r_H = 4.57$ Å and with 12 molecules as $r_H = 5.26$ Å. In the first case the equivalent hydration layer is 0.66 Å thick, and in the second one it is 1.35 Å thick. These results are different from the above-discussed thickness of 3−4 Å, which suggests that water molecules are not regularly distributed on the GMP surface. The water molecules are concentrated in the proximity of the phosphate groups, and the thickness of the hydration sphere represents the average water distribution. A similiar thickness of hydration layer (1.1 Å) was obtained by Fernandes,[41] who compared the hydrodynamic parameters of short DNA oligonucleotides in the "dry" and "hydrated" forms. The authors assumed the bead model where each atom of the nucleotide was represented by a single sphere of radius $\sigma = 2.8$ Å. Because the average van der Waals radius of the nucleic acid atoms is ≈1.7 Å, the difference was attributed to hydration.

In conclusion, the D_T measurements allow an estimation of the GMP hydrodynamic radius as $r_H = 5.37 \pm 0.36$ Å. The calculated radius of the maximally hydrated mononucleotide $r_H = 5.26$ Å is in good agreement with experiment. Therefore, the experimentally obtained radius r_H and the radius of each bead estimated from its value $\sigma = 4.75$ Å was applied in the bead model for the calculation of D_T coefficients of the structures formed by GMP. The presence of alkali metal ions stabilizes the stacks of G-quartets in a broad range of temperatures. At high temperatures D_T was measured for temperatures ranging from 10 to 80 °C. The GMP acid was studied in deionized water, pH 2; in solution of 100 mM NaCl, pH 5.5; in 10 mM Tris buffer, pH 7.3; and in 10 mM Tris buffer with 10, 20, and 50 mM NaCl, pH 7.3.

Errors. The percentage errors of the D_{T20} values, which varies for small concentrations (20, 40 mg/mL) from 1.5% to 6%, for medium concentrations (73, 111 mg/mL) from 0.5% to 4.5%, and for large concentrations (180, 260 mg/mL) from 0.5% to 6.5% are shown in the figures. The error bar symbols are of very small size, and very often their dimensions do not exceed the dimensions of the symbol. As for the errors coming from the established value of the sphere radius $\sigma = 4.75 \pm 0.29$ Å in the bead model (Figures 1 and 3), for example the difference of 0.3 Å in the single sphere radius gave the following percentage errors in calculated D_T value: for big molecules (stack of 16 G-quartets) ∼1.2%, for small molecules (G-quartet) ∼2.6%, and for single GMP monomer ∼6%. The error coming from the method resolution and therefore the time interval was of the order of 0.2 μs. The two molecules—GMP monomer and stack of two monomers—were distinguishable.

Temperature and Concentration Dependence. Translational diffusion coefficients D_T were measured as a function of temperature for six GMP concentrations in water: 20, 41, 73, 111, 180, and 261 mg/mL (the corresponding molar concentrations were 55, 113, 201, 306, 496, and 719 mM); see Figure 3a. The diffusion coefficient values calculated for 20 °C according to the bead model for different structures are shown by the dashed lines. The calculation was performed for a particular structure using the hydrodynamic radius of the monomer discussed earlier. The values of the translational diffusion coefficient D_T measured at temperature T (K) and solvent viscosity $\eta(t)$ are usually recalculated for respective values of D_{T20} at temperature 20 °C and water viscosity according to the formula

$$D_{T20} = D_T \frac{(293\ \mathrm{K})\eta(t, \mathrm{solvent})}{T\eta(20\ ^\circ\mathrm{C}, H_2O)} \qquad (7)$$

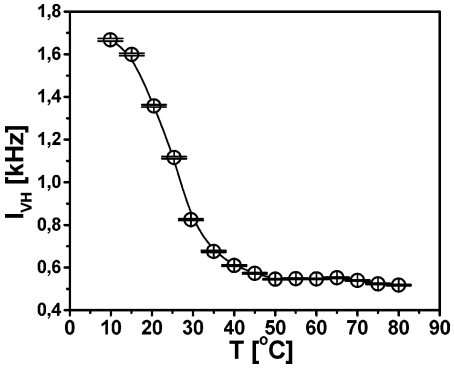

Figure 4. Intensity of depolarized component of scattered light I_{VH} as a function of temperature for GMP water solution of concentration $c = 177$ mg/mL, pH 2.

For GMP water solutions the correlation function is composed of a high-amplitude dominant component, which is shifting toward short times with increasing temperature. In the acidic solutions GMP forms a gel structure in which the G-quartets are arranged into four-string helices. At low temperatures and high concentrations of GMP, large structures appear. At 10 °C for the concentration of 261 mg/mL there are ordered associates composed of more than 32 layers of G-quartets. They decompose to stacks of seven quartets at 60 °C, while two-quartet stacks are observed for the concentration of 73 mg/mL at low temperatures and decompose to three GMP monomer stacks at 70 °C. A strong temperature dependence of the GMP structures in water solution is even more pronounced in Figure 3b. For GMP concentrations of 41 and 20 mg/mL (Figure 3a) only nucleotide monomers are observed. This observation is consistent with the results reported by Eimer and Dorfmüller.[29] The authors detected the formation of the G-quartets at concentrations above 54.5 mg/mL (150 mM). A comparison of D_T coefficient values suggests that the type of associates existing simultaneously in the solution is a function of temperature and GMP concentration. For example, a stack composed of seven G-quartets is formed at $T = 25$ °C for concentration $c = 180$ mg/mL and at $T = 60$ °C for concentration $c = 261$ mg/mL. At the same time, similar G-quartet stacks are observed at $T = 10$ °C for $c = 73$ mg/mL and at $T = 30$ °C for $c = 111$ mg/mL. For the sample concentrations of 261, 180, 111, 73, and 41 mg/mL the fast decomposition of the stack associates, observed at lower temperatures, is slowed starting from 40 °C and stops at higher temperatures (Figure 3b). It cannot be excluded that at low concentrations for which the interactions disappear all the stacks observed would decompose to single GMP monomers. Such an effect can be supported by the concentration dependence of D_{T20} at different temperatures. As indicated by the plot in Figure 3b, for high concentrations different structures are observed, depending on temperature. These structures disappear and only GMP monomers are observed at very low concentrations and high temperatures (common point in Figure 3b).

The melting curves which represent the intensity of the depolarized component of scattered light as a function of temperature, $I_{VH} = f(T)$, reflect also the process of temperature decomposition of GMP associates. Such measurements were performed for GMP in H_2O, $c = 177$ mg/mL, and the results are shown in Figure 4. As shown, in the temperature range of 10−50 °C with increasing temperature the order of the structures decreases and larger G-quartet stacks decompose to the stacks of two to three quartets. The occurrence of this process is also concluded from the plot of $D_{T20} = f(T)$, for $c = 180$ mg/mL, Figure 3a.

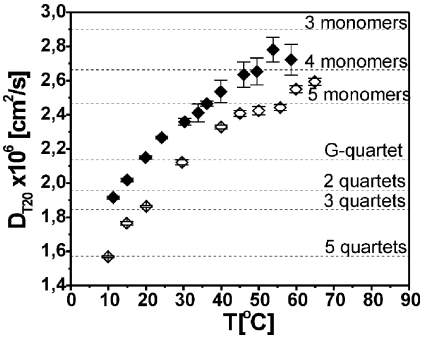

Figure 5. Translational diffusion coefficients D_{T20} as a function of temperature T for GMP (◊) in deionized water, pH 2, $c = 111$ mg/mL, and (♦) in 10 mM Tris buffer solution, pH 7.3, $c = 106$ mg/mL.

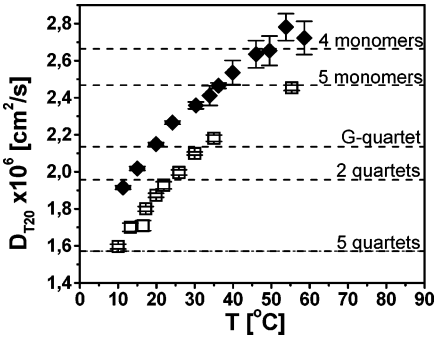

Figure 6. Translational diffusion coefficients D_{T20} as a function of temperature T for GMP concentration of (♦) $c = 106$ mg/mL in 10 mM Tris, pH 7.3, and (□) $c = 109$ mg/mL in 10 mM NaCl, 10 mM Tris buffer solution, pH 7.3.

Influence of pH. The size and stability of the stack associates formed were tested for three different hydrogen ion contents in solution, that is for pH 2, 5.5, and 7.3. For this purpose D_T was measured as a function of temperature in GMP solution of concentration $c = 106$ mg/mL, buffered by 10 mM Tris, pH 7.3, and in deionized water, pH 2. The results are shown in Figure 5, illustrating the influence of pH on the size and on the temperature of formation and decomposition of the structures. For example, at pH 2, $T = 10$ °C, five-quartet stacks are formed, whereas at pH 7.3 at the same temperature three-quartet stacks appear. However, at $T = 30$ °C, pH 2, stacks of seven GMP monomers were formed, and for pH 7.3 stacks of six monomers were formed from the G-quartets, which indicates formation of larger structures in low-pH solutions. At high temperatures the structures existing in both solutions (pH 2 and pH 7.3) will decompose into forms of equal hydrodynamic radius. These forms are four GMP monomer associates.

Sodium Ion Influence. In Figure 6 D_{T20} is plotted as a function of temperature for GMP concentration of $c = 109$ mg/mL, 10 mM Tris buffer, 10 mM NaCl. From the figure one can see that in the range 10−55 °C the five G-quartet stacks decompose to five GMP monomer stacks. The temperature decomposition of the structures created in water solution of pH 2 and in Tris buffer of pH 7.3 with addition of 10 mM NaCl is similar; see Figures 5 and 6. For pH 7.3, at the same temperature and at the same concentration of GMP, larger structures are formed when Na^+ is present in solution (Figure 6). The hydrodynamic radius calculated on the basis of the above-discussed data indicates the presence of the associates of four GMP monomers (Figure 5).

The concentration of hydrogen ions in GMP solution affects the size and stability of the structures formed, but this influence is smaller than that of the presence of sodium ions, as follows

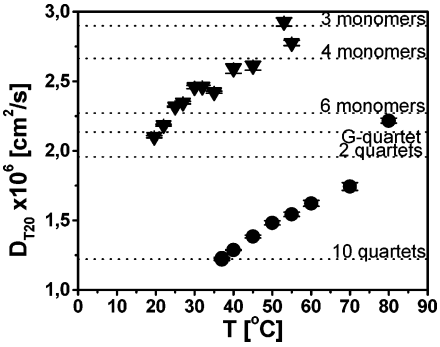

Figure 7. Translational diffusion coefficients D_{T20} as a function of temperature T for GMP concentration of (▼) $c = 83$ mg/mL in 50 mM NaCl, 10 mM Tris buffer solution, pH 7.3, and for GMP concentration of (●) $c = 89$ mg/mL in 100 mM NaCl, pH 5.5.

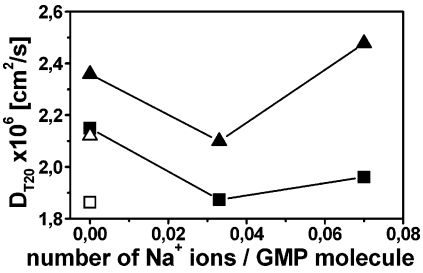

Figure 8. Diffusion coefficients D_{T20} as a function of sodium ions/GMP molecules ratio at pH 7.3 for (■) $T = 20$ °C and for (▲) $T = 30$ °C. Open symbols indicate for comparison the measurements at pH 2. The sample concentration varies from 104 to 111 mg/mL.

from a comparison of $D_T = f(T)$ measured for similar GMP concentration in 10 mM Tris buffer, 50 mM NaCl, pH 7.3, and in 100 mM NaCl, pH 5.5; see Figure 7. Figure 8 shows the diffusion coefficient D_T as a function of number of Na^+ ions per GMP molecule ratio. At the same pH the small amount of Na^+ ions (0.03 per GMP molecule) leads to formation of slightly bigger structures at both 20 and 30 °C in comparison to the situation when no sodium ions are present in solution. Further addition of Na^+ does not reinforce this effect and should be more carefully studied.

Figures 1 and 9 present the quartet and monomer structures, respectively. The D_T values calculated for these structures are listed in Tables 1 and 2.

IV. Conclusions

The translational diffusion coefficients, $D_T(T)$, and the intensity of the depolarized component of scattered light, $I_{VH}(T)$, were measured by means of photon correlation spectroscopy and depolarized light scattering, respectively. The measurements were performed as a function of temperature for water solution of GMP concentration $c = 20$, 41, 73, 111, 180, and 261 mg/mL and for sodium salt solution of GMP concentration $c = 83$, 89, 104, and 109 mg/mL.

The above methods allowed a simultaneous identification of single G-quartets or monomers and stacks of some tens of G-quartets or monomers in solution.

The hydrodynamic radius of GMP mononucleotide and the translational diffusion coefficient were determined as $r_H = 5.4$ Å and $D_T = 3.9 \times 10^{-6}$ cm^2/s. Assuming the bead model, the value of r_H was used for calculation of the hydrodynamic parameters of the structures formed by GMP.

In highly concentrated water solution GMP forms structures composed of associates of some tens of G-quartets (32 layers or more). Their size depends on the concentration of GMP and

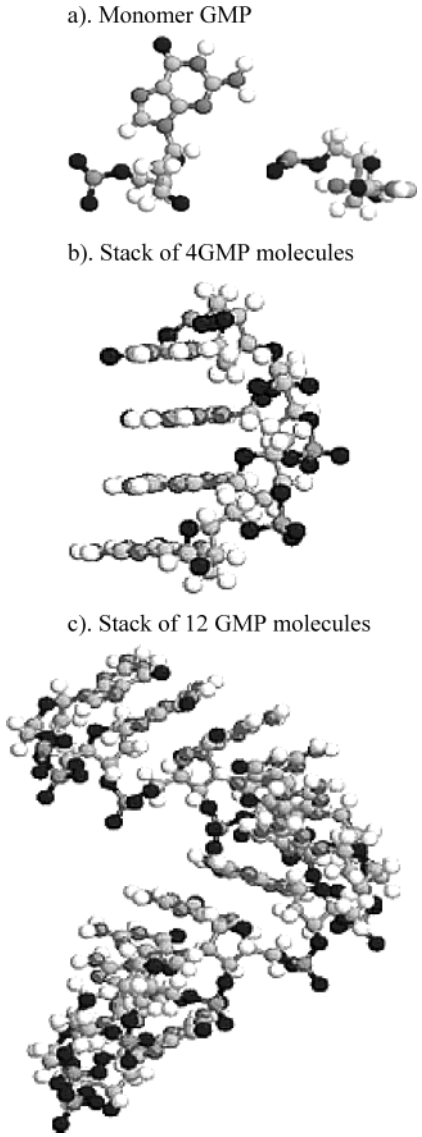

Figure 9. Structures of (a) GMP monomer nucleotide, (b) stack of four GMP molecules, and (c) stack of 12 GMP molecules presented as examples of associates formed due to stack interactions of guanine ring. The carbon atoms are light gray, nitrogen atoms are dark gray, oxygen atoms are black, and hydrogen atoms are white.

on temperature. With increasing temperature the G-quartet structures decompose and continuously transform to structures formed of single GMP monomers. In solutions with acidic pH values the G-quartet associates are larger than those formed in solutions with basic pH.

Sodium ions affect the size and stability of the structures formed. In solutions of the same pH, GMP concentration, and temperature, larger structures are formed in the presence of Na^+.

Stacks of four, three, and two G-quartets, characteristic of telomer DNA structures, are formed in solution of GMP concentration $c = 109$ mg/mL, in the temperature range 15−30 °C.

References and Notes

(1) Tougard, P.; Chantot, J.-F.; Guschlbauer, W. *Biochim. Biophys. Acta* **1973**, *308*, 9−16.

(2) Sasisekharan, V.; Zimmerman, S.; Davies, R. *J. Mol. Biol.* **1975**, *92*, 171−179.

(3) Zimmerman, S. B.; Cohen, G. H.; Davies, D. R *J. Mol. Biol.* **1975**, *9*, 181−192.

(4) Zimmerman, S. B. *J. Mol. Biol.* **1976**, *10*, 663−672.

(5) Franz, H.; Ciuchi, F.; Di Nicola, G.; De Morais, M.M.; Mariani, P. *Phys. Rev. E* **1994**, *5*, 395−402.

(6) Son, T. D.; Guschlbauer, W. *Nucleic Acids Res.* **1975**, *2* (6), 873−88.

(7) Sagan, B. L.; Walmsley, J. A. *Biochem. Biophys. Res. Commun.* **1985**, *128* (2), 980−986.

(8) Guschlbauer, W.; Chantot, J. F.; Thiele, D. *J. Biomol. Struct. Dyn.* **1990**, *8* (3), 491−511.

(9) Pinnavaia, T. J.; Marshall, C. L.; Mettler, C. M.; Fisk, C. L.; Miles, H. T.; Becker, E. D. *J. Am. Chem. Soc.* **1978**, *100*, 3625−3627.

(10) Detelier, C.; Laszlo, P. *J. Am. Chem. Soc.* **1980**, *102*, 1135−1141.

(11) Bouhoutsos-Brown, E.; Marshall, C.; Pinnavaia, T. J. *J. Am. Chem. Soc.* **1982**, *104*, 6576−6584.

(12) Fisk, L. C.; Becker, E. D.; Miles, H. T.; Pinnavaia, T. J. *J. Am. Chem. Soc.* **1982**, *104*, 3307−3314.

(13) Pinnavaia, T. J.; Miles, H. T.; Becker, E. D. *J. Am. Chem. Soc.* **1975**, *97*, 7198−7200.

(14) Borzo, M.; Detelier, C.; Laszlo, P.; Paris, A. *J. Am. Chem. Soc.* **1980**, *102*, 1124−1134.

(15) Walmsley, J. A.; Barr, R. G.; Bouhoutsos-Brown, E.; Pinnavaia, T. J. *J. Chem. Phys.* **1980**, *88*, 2599−2605.

(16) Kang, C.; Zhang, X.; Ratliff, R.; Moyzis, R.; Rich, A. *Nature* **1992**, *356*, 126−131.

(17) Chen, F.-M. *Biochemistry* **1992**, *31*, 3769−76.

(18) Sen, D.; Gilbert, W. *Nature* **1988**, *334*, 364−366.

(19) Daniels, G. A.; Lieber, M. R. *Nucleic Acids Res.* **1995**, *36*, 5006−5011.

(20) Evans, T.; Schon, E.; Gora-Maslak, G.; Patterson, J.; Efstratiadis, A. *Nucleic Acids Res.* **1984**, *12*, 8043−8058.

(21) Kilpatrick, N. W.; Torri, A.; Kang, D. S.; Engler, J. A.; Wells, R. D. *J. Biol. Chem.* **1986**, *261*, 11350−11354.

(22) Simonsson, T.; Pecinka, P.; Kubista, M. DNA tetraplex formation in the control region of c-myc. *Nucleic Acids Res.* **1998**, *26*, 1167−1172.

(23) Fry, M.; Loeb, L. A. *Proc. Natl. Acad. Sci. U.S.A.* **1998**, *91*, 4950−4954.

(24) Bell, G. I.; Selby, M. J.; Rutter, W. J. *Nature* **1982**, *295*, 31−35. (Shafer, R. H.; Smirnov, I. *Biopolymers* **2001**, *56*, 209−227.)

(25) Hammond-Kosack, M. C. U.; Dobrinski, B.; Lurz, R.; Docherty, K.; Kilpatrick, M. W. *Nucleic Acids Res.* **1992**, *20*, 231−236.

(26) Henderson, E.; Hardin, C. C.; Walk, S. K.; Tinoco, F., Jr.; Blackburn, E. *Cell* **1987**, *51*, 899−908.

(27) Williamson, J. R.; Raghuraman, M. K.; Cech, T. R. *Cell* **1989**, *59*, 871−880.

(28) Blackburn, E. H. Structure and function of telomeres. *Nature* **1991**, *350*, 569−573.

(29) Eimer, W.; Dorfmüller, Th. *J. Phys. Chem.* **1992**, *96*, 6790−6800.

(30) Provencher, S. W. *Comput. Phys. Chem.* **1982**, *27*, 213/229 (Schmitz, K. S. *An Introduction to Dynamic Light Scattering by Macromolecules*; Academic Press: San Diego, CA, 1990.)

(31) Berne, B. J.; Pecora R. *Dynamic Light Scattering with Applications to Chemistry, Biology and Physics*; Dover Publications: Mineola, NY, 2000.

(32) Tirado, M. M.; Garcia de la Torre, J. *J. Chem Phys.* **1979**, *71*, 2581−2588.

(33) Tirado, M. M.; Garcia de la Torre, J. *J. Chem Phys.* **1980**, *73*, 1986−1993.

(34) Banachowicz, E.; Gapinski, J.; Patkowski, A. *Biophys. J.* **2000**, *78*, 70−78.

(35) Rotne, J.; Prager, S. *J. Chem. Phys.* **1969**, *50*, 4831−4837.

(36) Rymden, R.; Stilbs, P. *Biophys. Chem.* **1985**, *21* (2), 145−156.

(37) Cantor, C. R.; Schimmel, P. R. *Biophysical Chemistry, Vol. II. Techniques for the Study of Biological Structure and Function*; W. H. Freeman and Co.: San Francisco, 1980.

(38) Schneider, B.; Cohen, D. M.; Schleifer, R.; Srinivasan, A. R.; Olson, W. K.; Berman, H. M. *Biophys. J.* **1993**, *65*, 2291−2303.

(39) Chalikian, T. V.; Sarvazyan, A. P.; Breslauer, K. J. *Biophys. Chem.* **1994**, *51* (2−3), 89−109. Chalikian, T. V.; Sarvazyan, A. P.; Plum, G. E.; Breslauer, K. J. *Biochemistry* **1994**, *33* (9), 2394−401.

(40) Schneider, B.; Patel, K.; Berman, H. M. *Biophys. J.* **1998**, *75*, 2422−2434.

(41) Fernandes, M. X.; Ortega, A.; Lopez Martinez, M. C.; Garcia de la Torre, J. *Nucleic Acids Res.* **2002**, *30* (8), 1782−1788.